Direct Selective Laser Sintering of High Temperature Materials

G. Zong, Y. Wu, N. Tran, I. Lee, D. L. Bourell, J. J. Beaman, and H. L. Marcus

Center for Materials Science & Engineering
and
Department of Mechanical Engineering
The University of Texas at Austin, Austin, TX 78712

Abstract

Selective Laser Sintering (SLS) involving a coexisting liquid and particulate solid during the SLS processing can be used to produce freeform parts directly with high temperature materials. Factors such as scanning laser power density, residence time, scan line spacing, the interfacial energies between the liquid and solid phases, powder bed biasing temperature, and sintering atmosphere greatly affect the microstructure evolution in the SLS process. Direct SLS of high melting temperature mixed powder materials was demonstrated using a 1.1 kW CO_2 laser SLS system. The relationship between the microstructures and the process parameters will be described.

1. Introduction

Selective Laser Sintering is a pressureless sintering process used for Solid Freeform Fabrication (SFF). SLS has been used successfully to fabricate prototype parts and preforms with polymer, ceramic, or low melting temperature metallic materials [1-4]. A liquid phase is usually involved during the SLS processes. The atomic diffusion in the liquid phase is faster than that in the concurrent solid state process. The capillary force due to a wetting liquid is the driving force for rapid compact densification. The liquid also reduces the interparticle friction; thereby, aiding rearrangement of the solid particles. In addition, liquid dissolution of sharp particle edges and corners may allow more efficient packing. Thus, SLS processing control offers the opportunities for microstructure manipulations to optimize properties. With proper control of the above parameters, direct SLS of materials is possible. In this paper, direct SLS of high melting temperature mixed powder materials will be demonstrated using a 1.1 kW CO_2 laser SLS system.

2. Experimental

To perform selective laser sintering of high temperature materials, a high power laser selective sintering system was designed and assembled. There are four major components in the system: 1) a 1.1 kw CO_2 laser system with focusing optics and scanning mechanism; 2) a

Sun station and its interface to control the laser pattern generation; 3) a sintering chamber with a resistance plate heater in part cylinder and inert gas purging capability; and 4) a powder delivery and leveling system. Figure 1 shows schematic diagram of the sintering cell.

The initial materials studied were Cu-Ni and WC-Co-Ni mixed powders as well as stainless steel 304L powders. Additive powders were also used. Optical metallograph, SEM, AES, EDS, and XRD were employed to study the sintering behaviors.
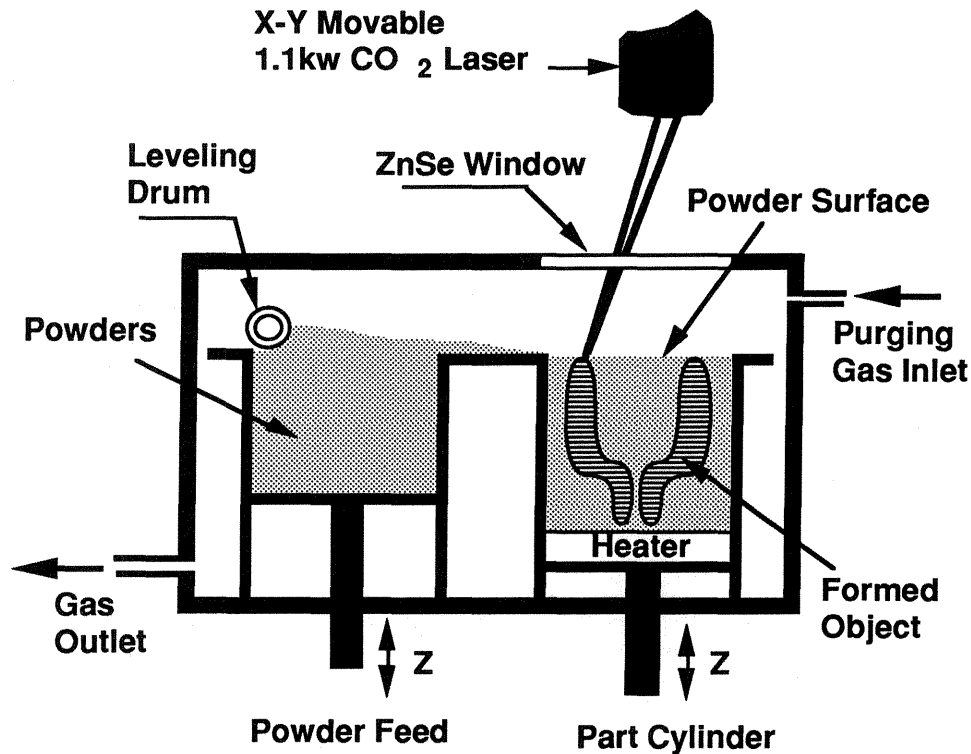

Figure 1 Sintering cell for high laser power SLS

3. Results and Discussions

The main SLS processing concerns are the properties of the starting powder, the laser parameter settings, and the atmosphere in which powder sintering occurs. These parameters and their interactions determine the SLS product quality. The initial results of the SLS of high temperature materials using the system described above will be presented with evaluation of laser parameter effects, role of additives, and sintering atmosphere effects.

3.1 Laser parameter effects in SLS

For a given SLS system, the laser parameters to be set in a typical SLS run are laser power density (P), scan speed (v), and scan spacing (S). Figure 2 shows the SLS sintering single layer thickness as a function of scan speeds and scan line spacing for 100 μm Cu powder. The sintered layer thickness decreases with increasing scan speeds due to shorter interaction (sintering) time. This thickness also decreases with decreasing scan line spacing. Since the laser beam diameter of 4.5 mm is larger than the scan line spacings studied (0.254, 0.508, 1.016, 1.270 mm), scan overlapping occurred in these tests. The smaller the scan line spacing, the more scan overlapping. Therefore, the sintered layer thickness decreases with increasing scan overlapping. This relationship can be explained by considering the fact that the thermal conductivity and reflectivity of the sintered solid are higher than those of the starting powder. The more the scan overlapping in a laser scan, the more laser energy will be transferred away by heat conducting through the sintered solid and reflected away by sintered solid surface. Thus the sintering layer thickness decreases.
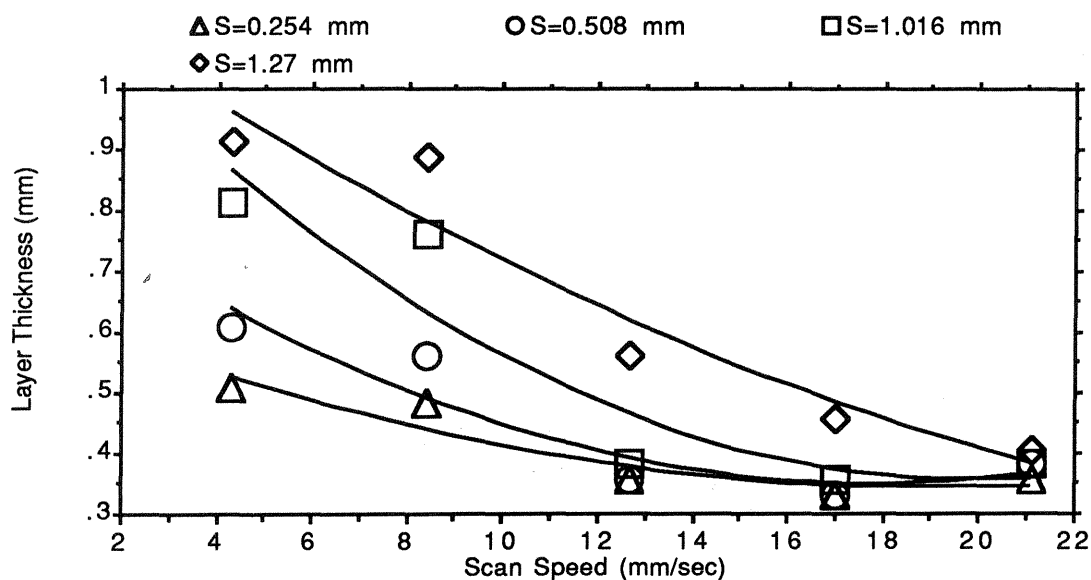
Figure 2 SLS sintering layer thickness as a function of laser scan speeds and scan line spacing. Laser power = 200w, beam size=4.5 mm, nitrogen flow rate = 60 l /min, no powder bed biasing temperature, for copper powder (~100μm) material.

To obtain a desired microstructure, sintering laser power (temperature) and scan speed (time) are the most important factors. The quality of the blend and analysis of the atmosphere also affect the microstructure. SLS tests and metallographic studies have been made to investigate the effect of laser power and scan speed on the sintering of a Bronze+Ni system. Figures 3 shows the typical sections of the SLS sintered part. These pictures show the strong effect of laser power and scan speed on the amount, size, and shape of residual porosity. The

sintered porosity is lower at higher laser power and lower scan speed. The pores become smaller and more rounded as the laser power increases and scan speed decreases because both sintering temperature and time are increased, more rearrangement [5] is involved during sintering. The metallographic study confirms the effect of laser power and scan speed. Figure 4 shows undersintered microstructure at conditions of Figure 3(a) and well sintered microstructure at conditions of Figure 3(c). Successful parts (Figure 5) with ~82% of theoretical density were obtained at laser power = 280w, beam size=4.5 mm, scan speed = 4.2mm/sec, scan line spacing =0.5mm, layer thickness=0.25mm, purging nitrogen flow rate = 60 l /min, powder bed biasing temperature=350 ^{0}C, for 60 wt% Bronze 9010 (~100μm)-30 wt% Ni (~100μm)-Cu3P (63μm) powder mixture.

During SLS process, laser heating causes temperature gradients that lead to the formation of residual stresses and strains throughout the sintered part. In the extreme case, these residual stresses will cause sintered layer curling. Laser power density and scan speed, together with scan path, part size, and powder bed biasing temperature, have strong effects on the generation of residual stresses in the sintered parts. Initial results showed that curling can be overcome or reduced by suitable setting these parameters. These results will not be discussed in detail in this paper.

3.2 Role of Cu3P in SLS of Cu-Ni materials

Tests have been carried out with several kinds of Cu-Ni and Bronze-Ni powders containing various amounts of Cu3P (0-10 wt%). These tests show that the present success of SLS of Cu-Ni powders is, to a large extent, dependent upon the addition of Cu3P. This section will discuss the role of Cu3P in SLS of Cu-Ni materials.
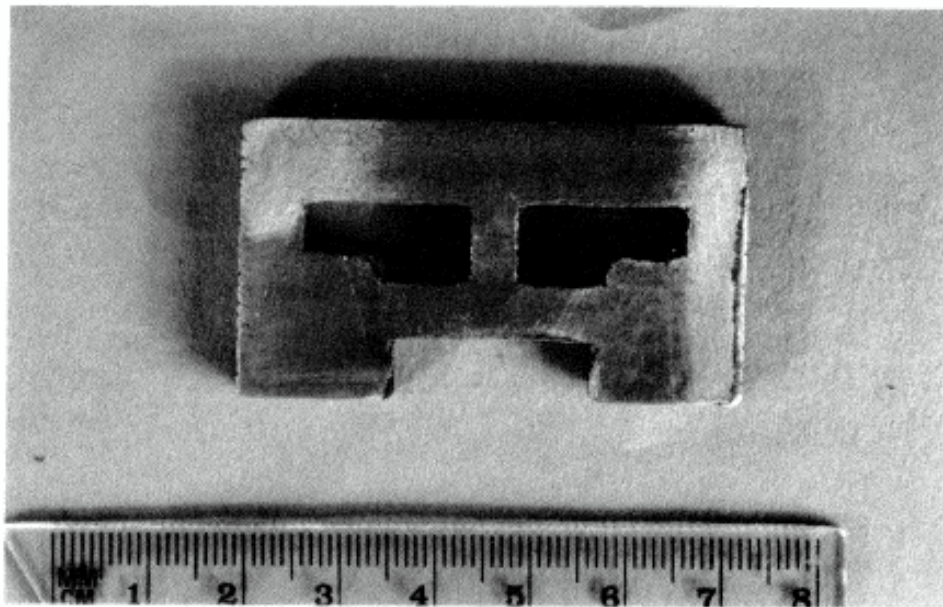
X-ray analysis of the starting powder mixture of 60 wt% Bronze-30 wt% Ni -Cu3P and its SLS sintered part indicated that Cu3P peaks showed up on the profile of the starting powder but not on the profile of SLS sintered samples (Figure 6). However, EDS analysis (Figure 7) showed that P is still in the sintered part. This phenomena can be explained by referring to the Cu-P equilibrium diagram [6] in Figure 8. The Cu-Cu3P partial system is a simple eutectic. The solubility of P in Cu is about 1.7 wt.% at the eutectic temperature of 714^{0}C. At the usual SLS sintering temperatures (above the melting point of copper, 1085 ^{0}C), Cu3P (melting point 1022^{0}C) will melt and there is considerable solubility of P in the molten copper. When Cu3P melted, P is diluted by the copper in bronze. Calculation indicates that total weight percentage of P in copper becomes 1.27%, about the solubility of P in copper at room temperature. Thus , after sintering, P is a solute in the Cu-P solution instead of forming Cu3P. Secondary electron micrograph and X-ray mapping of the fracture surface of the sintered 60 wt% Bronze-30 wt% Ni -Cu3P sample show P, Cu, and Sn elements appearing at same area of the sintered part, revealing P-Bronze solution (Figure 9). Figure 9 also shows that Ni remained solid during the sintering, as seen earlier in the optical microscopic studies (Figure 4).
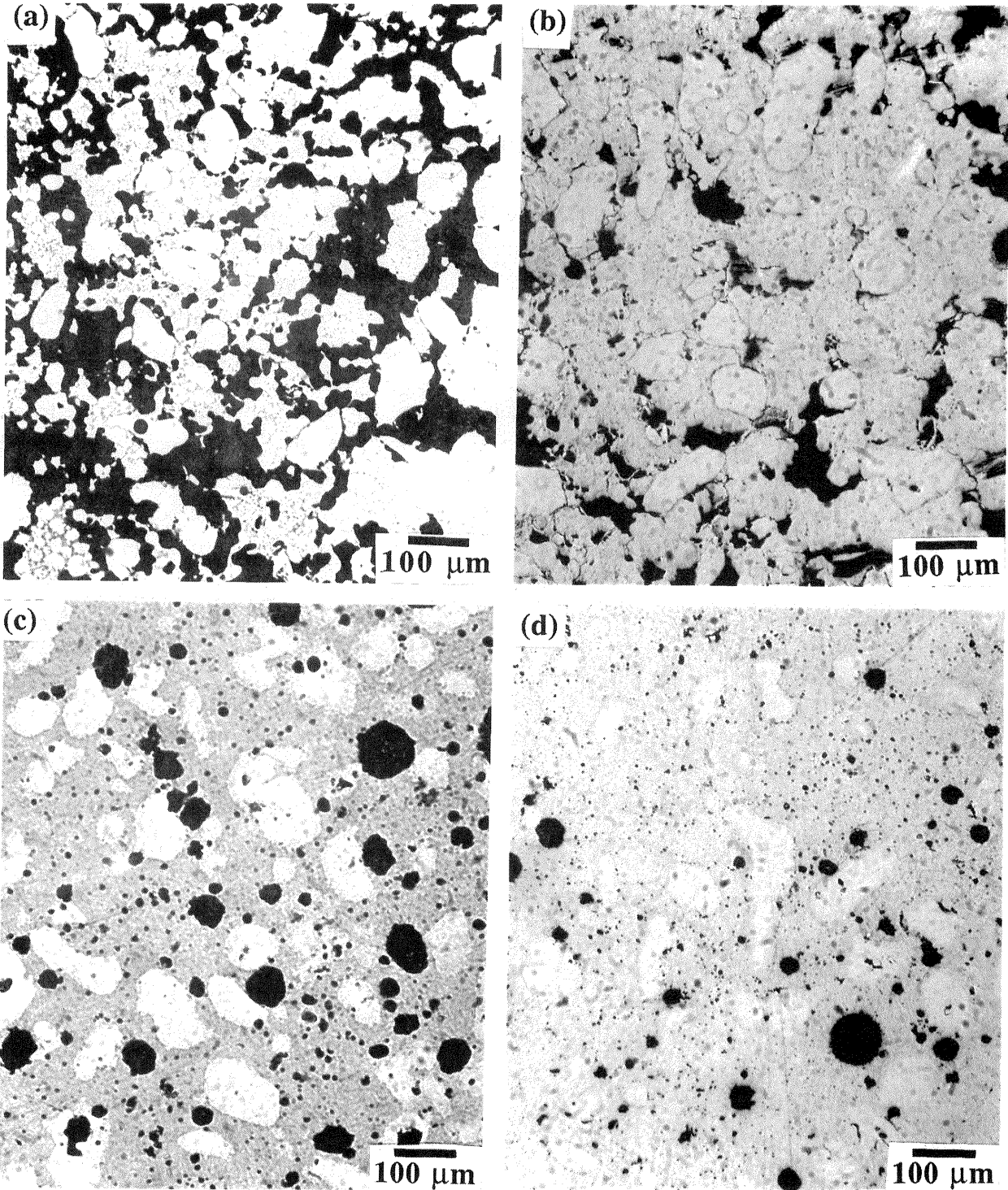
Figure 3 Microstructure of Bronze+Ni+Cu3P sintered at laser beam size=4.5 mm, scan line spacing =0.5mm, purging nitrogen flow rate= 60 l /min, no powder bed biasing temperature, and (a) laser power = 200w, scan speed = 21.2mm/sec, (b) laser power = 200w, scan speed = 12.7mm/sec, (c) laser power = 280w, scan speed = 21.2mm/sec, (d) laser power = 280w, scan speed = 12.7mm/sec.
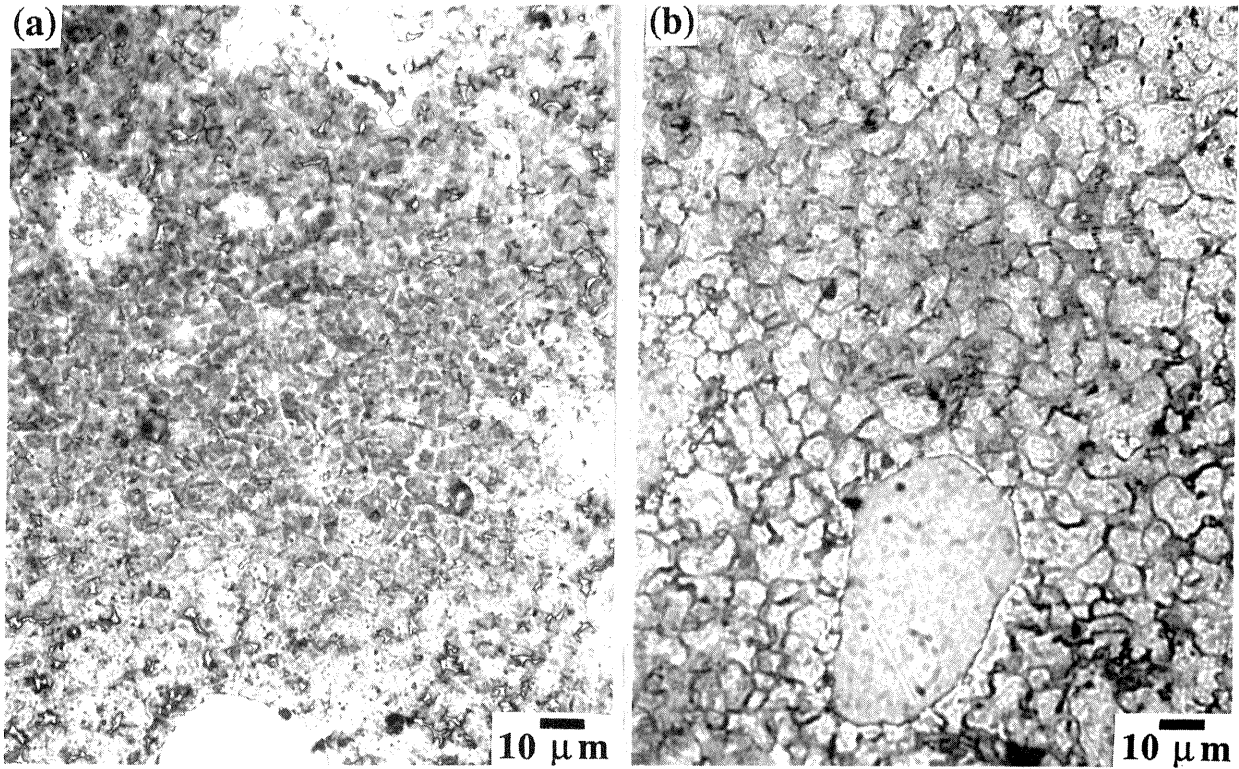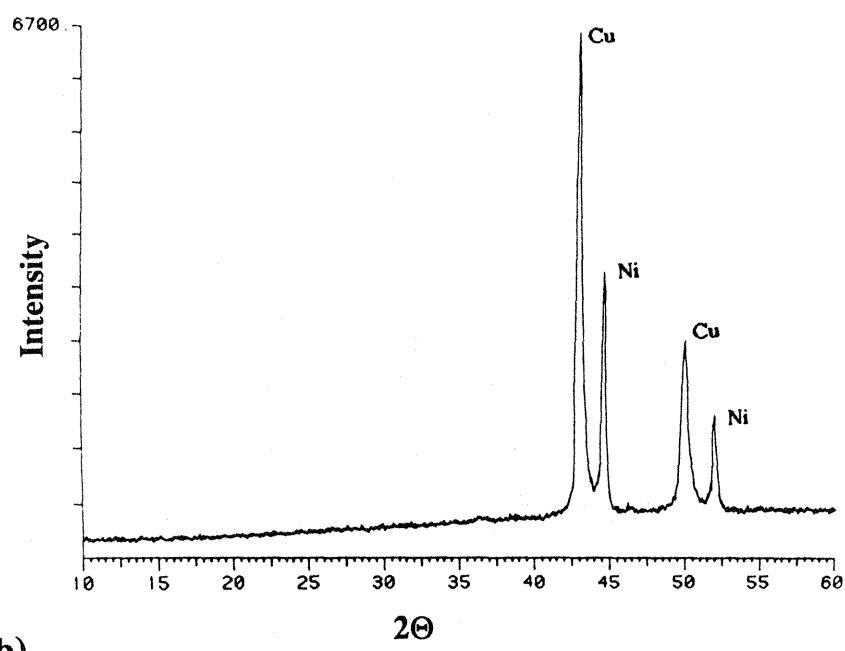
Figure 4 Microstructure of Bronze+Ni+Cu3P sintered at laser beam size=4.5 mm, scan speed = 21.2mm/sec, scan line spacing =0.5mm, purging nitrogen flow rate= 60 l /min, no powder bed biasing temperature, and (a) laser power = 200w, (b) laser power = 280w.

Figure 5 SLS Cu-Ni part.
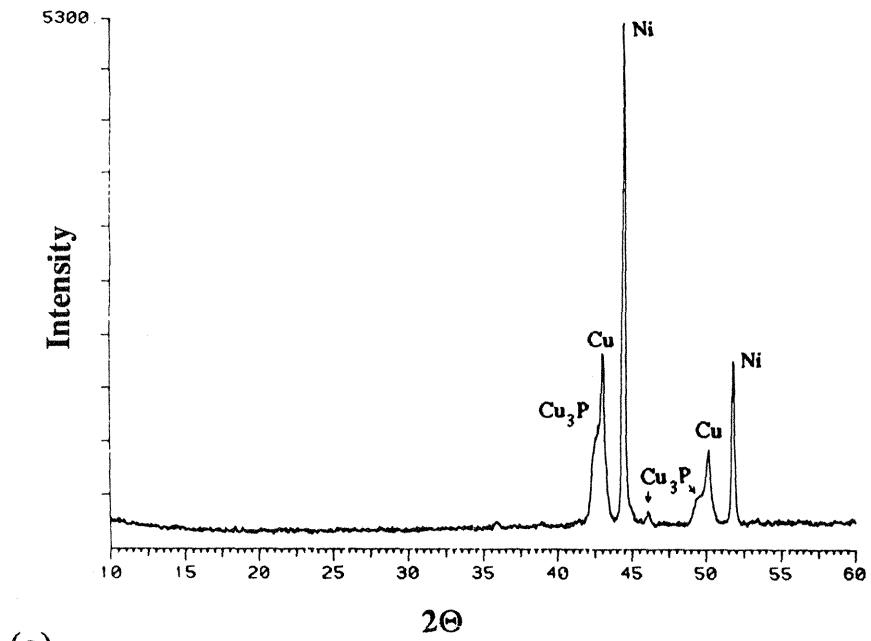
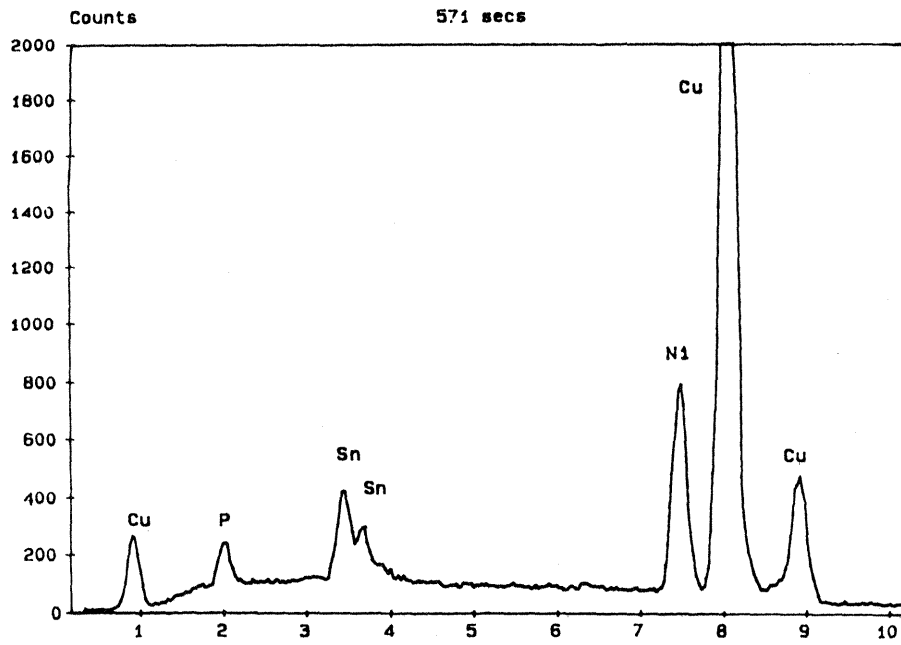Figure 6 X-ray profiles of (a) starting powder mixture and (b) SLS sintered 60 wt% Bronze-30 wt% Ni -Cu3P.

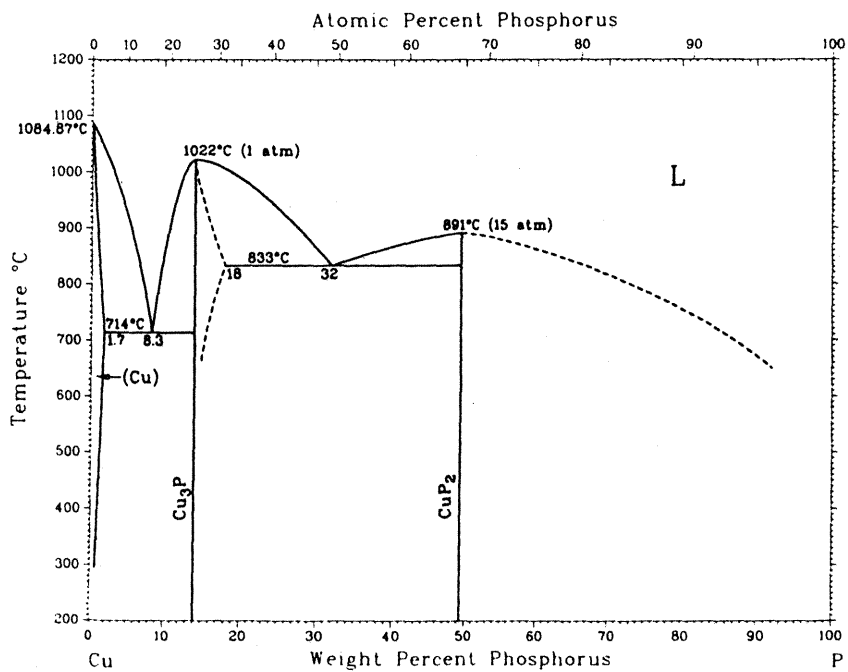Figure 7 EDS analysis of SLS sintered 60 wt% Bronze-30 wt% Ni -Cu3P.

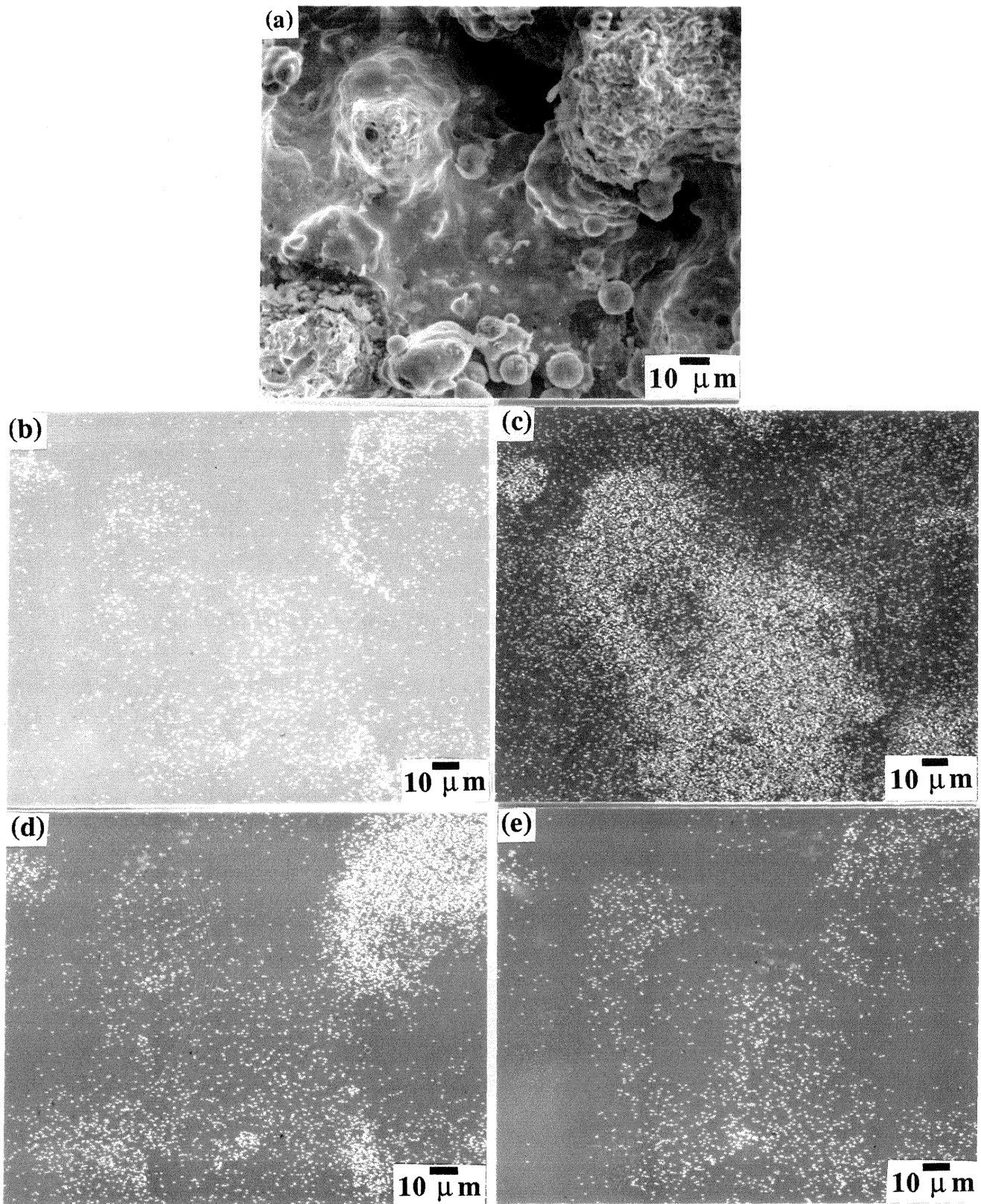Figure 8 Cu-P equilibrium diagram [6].

Figure 9 The secondary electron image (a) and X-ray element maps of (b) P, (c) Cu, (d) Sn, and (e) Ni form the fracture surface of the SLS sintered 60 wt% Bronze-30 wt% Ni -Cu₃P.

Having located P in the sintered samples, we now discuss the role of P/Cu3P in the SLS process. Smooth sintering layers (less balling) can be obtained when Cu3P is added to the powder mixture. Therefore, the present of P in the SLS process may enhance sintering by improving the wettability of Cu-Ni system through reducing surface tension of liquid copper. Since the free energy of formation of P oxide is much smaller (more negative) than that of Cu and Ni, P may also act as a localized oxygen 'getter' and partially prevent the oxidations of Cu and Ni, thus enhance sintering. In-situ Auger fracture analysis of the fracture surface of SLS sintered 60 wt% Bronze-30 wt% Ni -Cu3P sample revealed strong oxidation and high P content in the oxide (Figure 10), though no wetting problems occurred during the sintering process. The carbon peak originates from the carbon on the free surface of the pores. This analysis supports the idea that P is a localized oxygen 'getter'. Systematic investigations into the effects of P and other wetting additions on the sintering behavior of Cu-Ni system in an oxygen clean environment are highly desirable.

3.3 Sintering atmosphere effects in SLS

The sintering atmosphere is one significant factor affecting selective laser sintering, especially high temperature SLS. The atmosphere protects against surface contamination during sintering. Additionally, a cleaning function is desired from the atmosphere to remove films (for example oxides) for rapid melt flow. The atmosphere plays an important role in reducing surface films which can alter the wetting angles. In conventional liquid phase sintering, best densification and properties can be achieved using vacuum sintering in many systems [5]. Residual atmosphere can be trapped in pores which seal during liquid flow. Such trapped atmosphere inhibits full densification. Sintering in an inert or insoluble atmosphere is most detrimental for this reason. The present SLS system uses an inert gas purging system to reduce the surface layer contamination. This section will address some problems associated with such an approach.

Residual gas analysis (RGA) was performed to analyze the gas in the working chamber. With 60 l /min nitrogen purging, which is the setting for all tests discussed in the paper, the N_2 to O_2 partial pressure ratio 5000:1 was measured. SLS of stainless steel 304L powder was unsuccessful using such an environment due to the oxidation problem.

SLS of WC-Co-Ni system produced strong parts with rough surfaces (Figure 11). Wetting angle of WC by both liquid Co in hydrogen and liquid Ni in vacuum at 1500°C is 0 [7]. However, the oxidation of Co and Ni causes poor wetting and thus balling. Auger surface analysis of sintered 70 wt.% (WC-12Co)-20 wt.% Co- Ni showed oxygen in the sample, as seen in Figure 12. For a sintered layer, balling occurs on the top of the layer, and the bottom of the layer shows good wetting. Optical studies of the bottom of the layers revealed expected composite microstructure (Figure 13a), and WC wets well by metal matrix Co and Ni. The

study implies that the oxidation of Co and Ni occurs only on the liquid surface during the SLS process. Figure 13b shows the fracture surface of the sintered WC-Co-Ni sample, where voids with liquid pools are obvious. These voids may be introduced by N2 gas trapped in liquid during liquid flow in SLS processing.
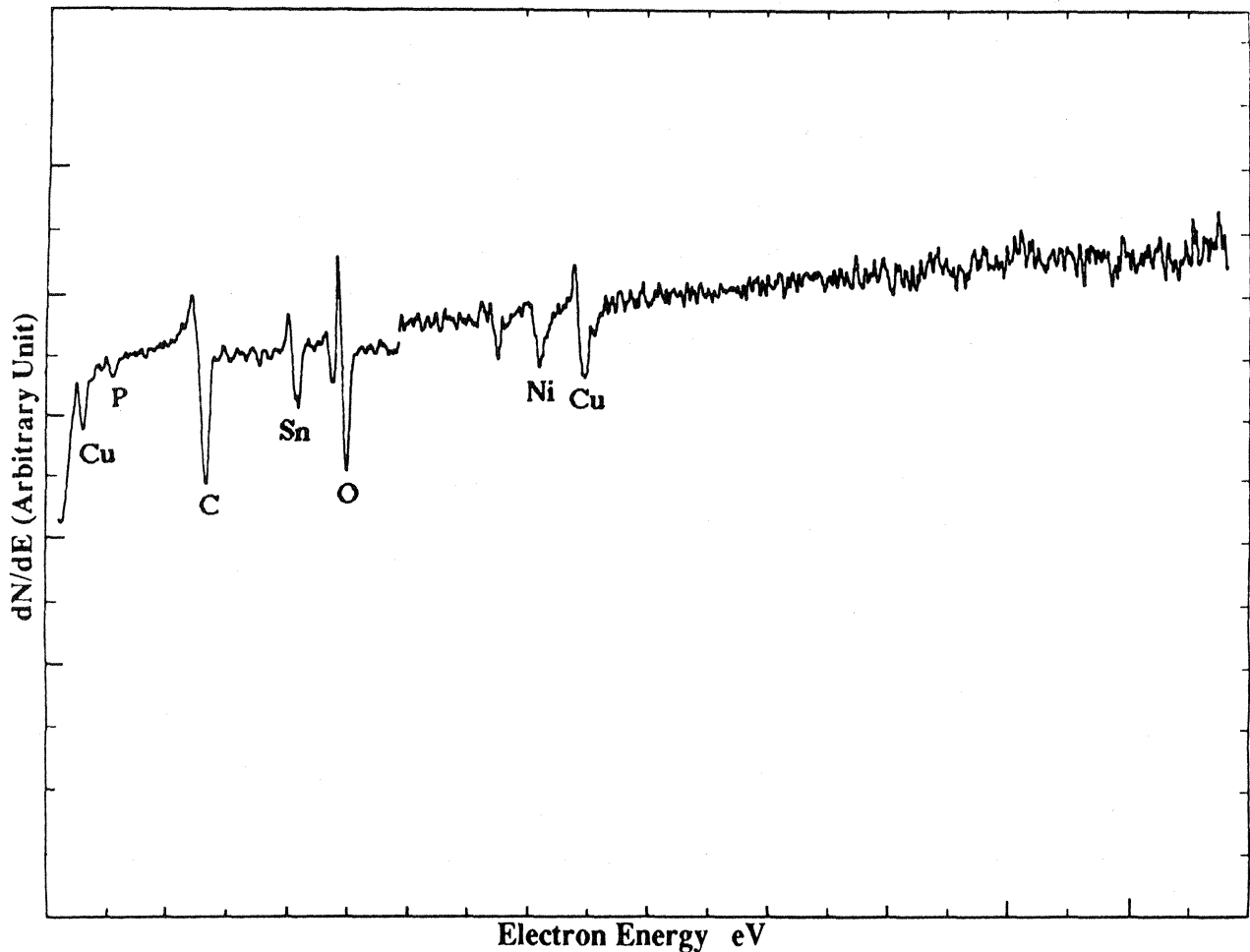

Figure 10 AES analysis of the in-situ fracture surface of the SLS sintered 60 wt% Bronze-30 wt% Ni -Cu3P.

4. Summary

Direct Selective Laser Sintering of high temperature powder mixtures has been demonstrated. Initial results indicate that SLS involving a coexisting liquid and particulate solid during the sintering can be used to produce freeform parts directly with high temperature materials. Many factors including scanning laser power density, residence time, scan line spacing, powder bed bias temperature, atmosphere, interfacial energies between the liquid and solid phases, and roles of additives are discussed in terms of the microstructure evolution.

These parameters and other factors such as solid phase solubility in the liquid, relative penetration of the liquid, particle size and distribution, powder leveling thickness and density are still to be studied.
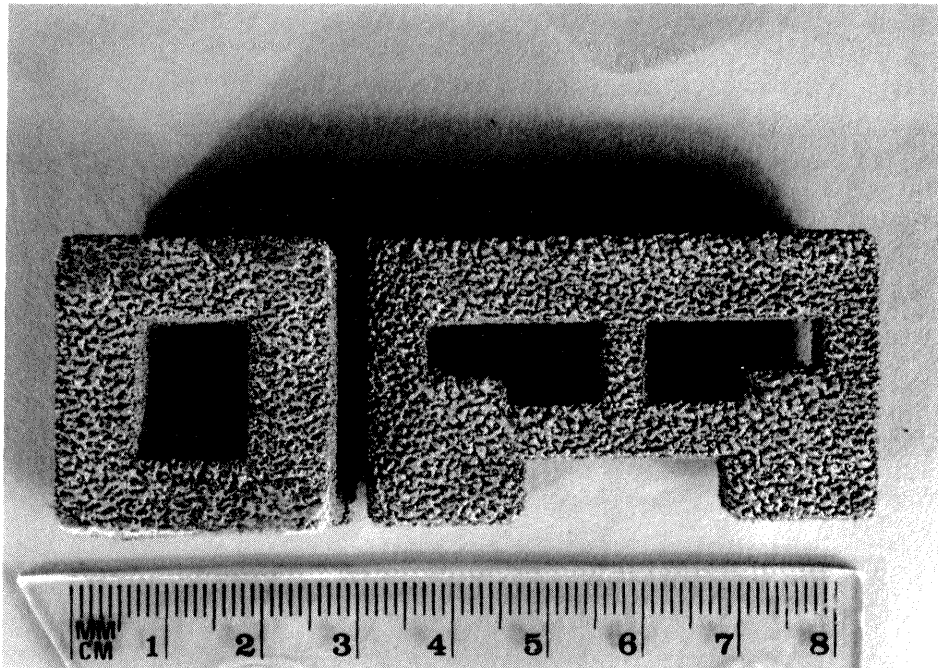

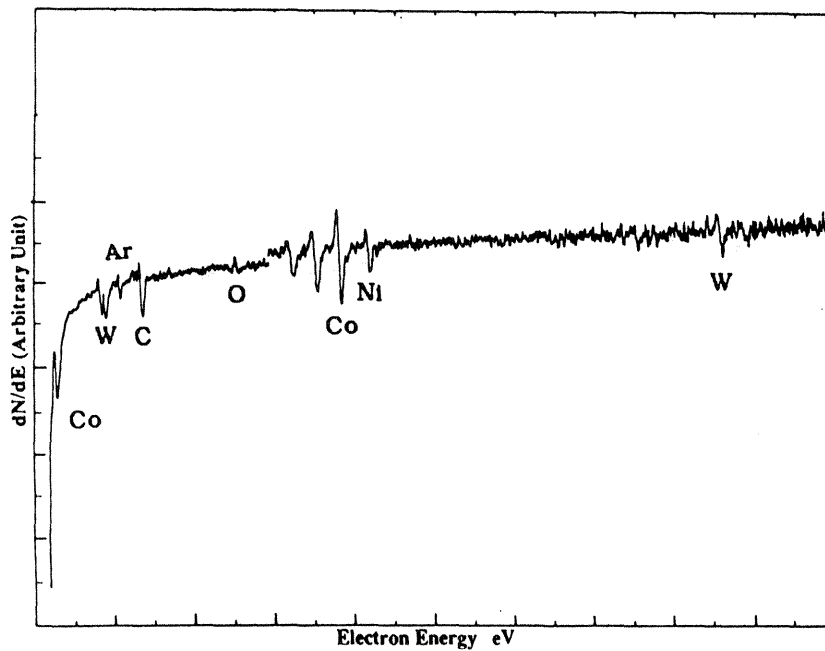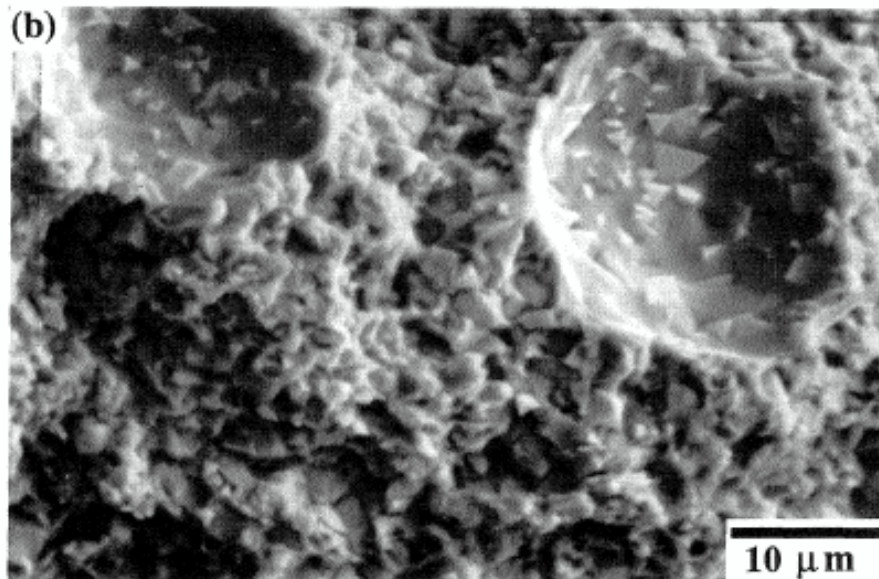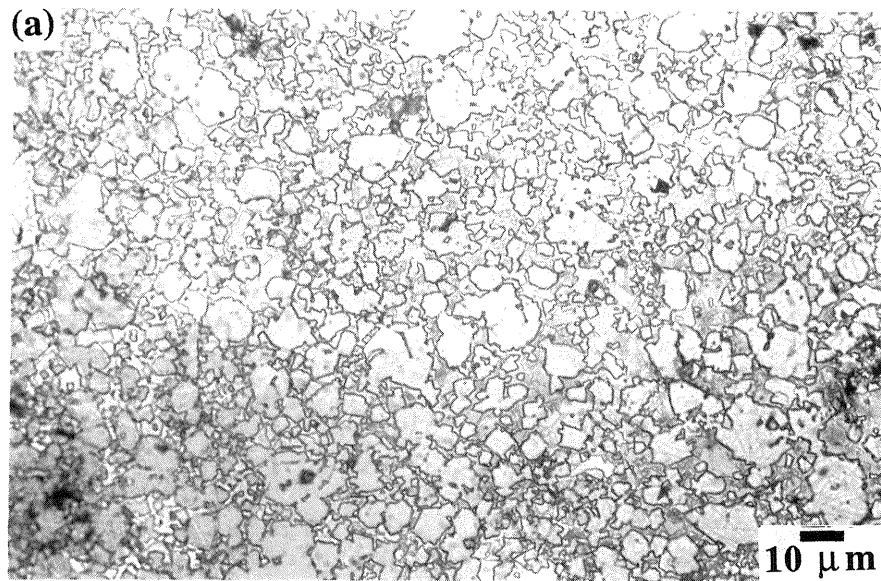**Figure 11** SLS fabricated WC-Co-Ni parts.

Figure 12 AES analysis of the (WC-12 wt.% Co)-20 wt.% Co-10 wt.% Ni sample, sputtering time = 6min.

Figure 13 (a) Optical and (b) SEM micrographs of SLS sintered (WC-12 wt.% Co)-20 wt.% Co-10 wt.% Ni sample.

Acknowledgement

References

1. <u>1990 Solid Freeform Fabrication Symposium Proceedings</u>, Edited by J.J. Beaman, H.L. Marcus, D.L. Bourell, J.W. Barlow, 1990, The University of Texas at Austin, Austin, Texas.
2. <u>1991 Solid Freeform Fabrication Symposium Proceedings</u>, Edited by H.L. Marcus, J.J. Beaman, J.W. Barlow, D.L. Bourell, R.H. Crawford, 1991, The University of Texas at Austin, Austin, Texas.
3. H. L. Marcus, J. J. Beaman, J. W. Barlow, and D. L. Bourell, "Solid Freeform Fabrication: Powder Processing," *Ceramic Bulletin*, 69(6), 1990, 1030-31.
4. D. L. Bourell, H. L. Marcus, J. W. Barlow, and J. J. Beaman, "Selective Laser Sintering of Metals and Ceramics," to be published in the October 1992 issue of the *International Journal of Powder Metallurgy*.
5. Randall M. German, <u>Liquid Phase Sintering</u> (New York, NY: Plenum Press, 1985), 127-151.
6. "Binary Alloy Phase Diagrams," second edition, ASM International, 1990 Vol. 2, T. B. Massalski, editor-in-chief.
7. G. S. Upadhyaya, "Wetting of Ceramics by Melts - An Electronic Approach," <u>Sintered Metal-Ceramic Composites</u>, edited by G. S.. Upadhyaya, Elsevier Science Publishers B.V., Amsterdam 1984, p. 41.